



SENSE ROADMAP

Table of Contents

1. Executive Summary.....	4
2. Overview of SENSE.....	5
3. The State of the Art.....	7
3.1. PMTs.....	7
3.2. SiPM.....	7
3.3. Other Sensors.....	8
3.4. Critical Parameters.....	8
4. SiPM.....	10
4.1. Performance of Sensors.....	10
4.2. Readout Electronics.....	11
4.2.1. Developments in Application-Specific Integrated Circuits (ASICs) for SiPM Readout...	11
4.2.2. Digital sensors.....	12
4.3. Integration.....	12
4.4. Simulation & Modelling SiPMs.....	14
4.4.1. Numeric simulation of Geiger avalanche multiplication process in Silicon.....	14
4.4.2. Modelling of reverse current-voltage characteristic of SiPM.....	14
4.4.3. Modelling of sensor as signal source.....	15
5. Classical PMTs.....	16
5.1. Quantum Efficiency.....	17
5.2. The State of the Art of Quantum Efficiency in PMTs.....	17
5.3. Photo Electron Collection Efficiency.....	19
5.4. Photon Detection Efficiency.....	20
5.5. First Dynode Amplification: A Key to Amplitude Resolution.....	20
5.6. Transit Time Spread.....	21
5.7. Afterpulsing.....	21
5.8. Single Photo Electron Peak to Valley Ratio.....	22
5.9. Influence of the Earth's Magnetic Field on the PMT Gain.....	22
5.10. Typical Achieved Parameters For the Recent Generation of Small-Size PMTs.....	22
6. SENSE Contributions to R&D of Sensors.....	25
6.1. SENSE Contributions to SiPMs.....	25
6.1.1. Performance of Sensors.....	25
6.1.2. Matrices of SiPM.....	27
6.1.3. The D-LIGHT development.....	28
6.2. SENSE Contributions to PMTs.....	30
7. Strategy.....	31
7.1. SiPM.....	31
7.2. PMT.....	32
7.3. Milestones.....	33
8. Summary.....	34
9. Bibliography.....	35

LIST OF TABLES AND FIGURES

TABLE 1. COMPARISON OF BASIC PARAMETERS.....	9
TABLE 2. TECHNICAL SPECIFICATION.....	24
TABLE 3. MAIN CHARACTERISTICS OF BEST BIALKALI PMTs AS OF TODAY.....	32
FIGURE 1. PHOTO OF CANDIDATE PMTs FOR CTA.....	16
FIGURE 2. QE MEASURING CUSTOM-DESIGNED DEVICE IN MPI.....	17
FIGURE 3. THE MEASURED QE OF SIX EXPERIMENTAL PMTs.....	18
FIGURE 4. PEAK QE OF 300 PMTs PRODUCED BY HAMAMATSU IN 2013.....	18
FIGURE 5. GAIN VERSUS APPLIED HV FOR THE HAMAMATSU 7-DYNODE AND 8-DYNODE PMTs.....	23
FIGURE 6. PMT PULSE WIDTH VERSUS APPLIED HV DISTRIBUTION FOR HAMAMATSU AND ETE PMTs.....	23
FIGURE 7. PMT PULSE WIDTH VERSUS GAIN (APPLIED HV) FOR HAMAMATSU AND ETE PMTs.....	23
FIGURE 8. PULSE WIDTH OF A HAMAMATSU 7-DYNODE PMT OPERATED UNDER 1000 V.....	23
FIGURE 9. CROSS-CHECK OF PDE AS A FUNCTION OF OVERVOLTAGE AT 405 NM WAVELENGTH, BETWEEN THREE PARTNERS.....	26

1. Executive Summary

This Roadmap aims to define the R&D activities that SENSE would like to follow for the development of the ultimate low light-level sensor(s), mainly for future astroparticle physics projects, but as well for other applications, e.g. in medical industries. In this document, we focus on developments that are crucial for two photo-sensing technologies; silicon photomultipliers (SiPMs) and photomultipliers (PMTs). We have identified three major sectors of development for each technology: (1) the performance of the sensors (which usually depends on the application), (2) the readout/control electronics, and (3) the integration of such electronics into the sensor. For each sector, we point out the specifications required to address individual fields of application, which challenges must be overcome. In addition, the results of ongoing specific R&D activities taking place in line with the roadmap idea within SENSE are presented.

2. Overview of SENSE

The primary objectives of SENSE are to develop a European R&D roadmap towards the ultimate low light-level (LLL) sensors, to monitor and evaluate the progress of the developments with respect to the roadmap, and to coordinate the R&D efforts of research groups and industry in advancing LLL sensors. In addition, SENSE aims to liaise with strategically important European initiatives and research groups and companies world-wide, to transfer knowledge by initiating information and training events and material, and to disseminate information by suitable outreach activities.

A coordination of European research groups actively working with LLL sensors is currently missing. On a technology forum on photosensors and auxiliary electronics organized in 2010 in the frame of the ERA-NET ASPERA-2, representatives from academia and industry pointed out that developments could be made faster when one or a few leading labs could take the initiative, to drive these activities, and to work in close collaboration with a wide range of interested research groups and industries. This attitude has a central role in SENSE. By formulating a **roadmap** incorporating all the major R&D activities necessary for the development of the ultimate LLL sensors, the R&D efforts of European research groups, along with industrial and strategic partners worldwide, will be efficiently aligned and significantly strengthened. Such **coordination** shall clearly underline and focus on the most promising developments with unified efforts. The **competition** between groups shall be stimulated in those cases when key developments can be accelerated.

The project aims at merging know-how of primarily European experts in developing the ultimate LLL sensors and taking the leadership in these R&D activities. Following new and emerging technologies in detecting minimal quantities of light (single photons) is a challenge. However, the **close cooperation between industry and academia** in several research disciplines can become an ideal partnership for developing substantially improved LLL sensors that can find immediate application in research projects as well as become commercial products.

European companies shall be supported in getting to know the latest developments during the technology fora and meetings with developers, experts, and young talented researchers with interest in technology development. This will help European companies to be competitive concerning first-class LLL devices as well as with applications making use of the most efficient LLL sensors.

Given that many LLL-sensor applications are in the field of medical diagnostic, the substantial improvement in LLL-sensor technology will have a **clear positive societal impact** if the radiation doses for patients can be significantly reduced.

The **innovation potential** is enormous when it comes to a replacement of PMTs by the new SiPM technology. PET scanners could then be integrated into MRIs and allow for studying structures and functional activities in vivo, which is important for cancer research, Alzheimer studies, and drug tests. With the current state-of-the-art technology, such a combined diagnostic seems to be problematic. **Miniaturization** and **cheaper mass**

production of significantly improved LLL sensors will definitely lead to a wealth of innovative products in the long-term.

This document is the product of the roadmapping process, which was intensively discussed during the recent LIGHT-2017 workshop with experts in the area of LLL sensors. This document has to be further developed, applied and in the future also monitored.

The SENSE Consortium has four partners (Deutsches Elektronen Synchrotron/ DESY-Germany, University of Geneva/ UNIGE - Switzerland, Max-Planck Institute for Physics - Germany, Karlsruhe Institute of Technology/ KIT - Germany) and has involved several international working groups performing on a basis of a cooperation agreement as well as an international group of experts engaged from the broad community.

The duties of the Consortium are structured into five work packages. The Roadmap falls under Work Package 1 and is under the lead of the Max-Planck-Institute for Physics.

3. The State of the Art

All innovation with respect to LLL sensors is driven by the challenging demands by research projects and infrastructures. Currently, with about 600000 PMTs/year, medical diagnostic instrumentation is the largest consumer of PMTs, where they are used in Positron Emission Tomographs (PET), in Gamma cameras, and in many applications in life sciences. Besides specific applications of PMTs, e.g. in the oil drilling industry, large-scale experiments in basic research are consumers of up to several 100000 LLL sensors, albeit the net consumption varies from year to year. The demand to reach higher and higher levels in light detection with the highest precision and efficiency in astroparticle, particle, and nuclear physics experiments is one of the main R&D drivers in the domain of the LLL detection.

The market for LLL sensors in the context of future upgrades of Astroparticle Physics projects is huge - it was estimated in 2010 that about 0.5 Billion € should be spent in the next decade. SENSE is currently working to evaluate existing infrastructures with major upgrades, upcoming projects, and their timeframes. The work (within the SENSE project) will be finalized and discussed during a Technology Forum in first half of 2018.

We now give a brief overview of three categories of photosensors (PMT, SiPM, and other) and summarize the improvements in performance.

3.1. PMTs

PMTs are produced by companies in various sizes, from very small (below 1 cm in size) to very large (up to 50 cm Ø). PMTs selected from Hamamatsu for the Cherenkov Telescope Array (CTA) project are now confirming the expected high quality performance of these devices. Measurements show substantially better performance of these devices than the requirements for parameters such as QE, afterpulse rates, and Peak/Valley ratio of single photon counting set by the CTA collaboration. However, the number of companies worldwide is relatively small (≤ 5), which impairs fruitful competition.

3.2. SiPM

SiPM technology was first used in astroparticle physics experiments (e.g., in very high energy imaging Cherenkov telescope gamma-ray cameras, for read-out of scintillator detectors, and dark matter experiments). A few examples are the FACT camera, the imaging cameras of the three different Small Size Telescopes (SST) of the CTA collaboration (SST-1M, ASTRII, GCT) and of the Schwarzschild-Couder Middle Size Telescope (MST) along with a SiPM-based sensor clusters for the MAGIC telescope project, which are under extensive tests and evaluation. First prototypes are in the test phase for SiPM-based fluorescence cameras (EUSO-Balloon, FAMOUS at Auger) and for light detection in future Dark Matter experiments (Dark Side, DARWIN).

Currently, a large variety of SiPM matrices are available in the sensor market. There also exist a variety of alternative commercial readout solutions. SiPM matrices with improved

filling factor are currently being developed to overcome the low geometrical efficiency of these devices. However, for fast timing applications the size of SiPMs is limited to several mm, because of the charge collection time. Furthermore, increased cell size would unfortunately increase its gain along with the undesirable crosstalk.

SiPM-based matrices with complete readout, like in a CMOS (or in a CCD) camera, will be scalable and would allow a simple assembly in arbitrary shape, arriving to large coordinate-sensitive imaging camera. However, stray heat might cause a problem in fast on-chip digital readout solutions. Comparative studies of PMT and SiPM solutions already indicate comparable photon-detection efficiencies, albeit a higher signal-to-noise ratio for PMTs.

3.3. Other Sensors

Cryogenic PMTs are currently the standard light sensors applied in dark matter searches using liquid Argon and Xenon (LAr and LXe, respectively). In addition to standard requirements, such as high QE, low DCR and stable performance, these PMTs need to be optimized concerning a very low radioactive contamination. Low Uranium and Thorium content is necessary to suppress any neutron background.

Gaseous PMTs (GPMs) are explored as alternative in LLL detection in cryogenic applications. This technology may provide a high filling factor and may allow to fully surround an experiment and to detect light in all directions. First measurements with 4" GPMs demonstrate a large dynamic range, good stability, energy and time resolution as well as a low DCR.

The GERDA experiment uses a combination of conventional and novel light detectors and is thus the first experiment with a large SiPM array operated at cryogenic temperature.

The successful application of a tungsten transition-edge sensor (TES) operated below 100 mK in the Any Light Particle Search-II (ALPS-II) experiment to detect single photons in the near-infrared demonstrates that this technology is entering astroparticle physics. One can speculate that further R&D may help this promising low-background single-photon detection technology to find wider application in research.

Several developments of optical modules for high-energy neutrino experiments have been presented, as single and multi-PMT designs. Prototyping for a completely new design, a wavelength-shifting optical module (WOM), has been presented, but further R&D is required to demonstrate the performance of this innovative design.

3.4. Critical Parameters

Table 1 provides a comparison of basic parameters for PMTs and SiPMs available in 2010 and 2015, where the improvements of both technologies are clearly demonstrated.

	2010	2015
PMT		
Peak Quantum Efficiency (QE)	28-34%	36-43%
Photo Electron Collection Efficiency on the 1 st Dynode	60-80%	94-98%
Afterpulse Rate (for a set threshold ≥ 4 photo electrons)	0.5%	< 0.02 %
SiPM		
Peak Photon Detection Efficiency (PDE)	20-30%	50-60%
Afterpulse Rate	30-40%	< 2%
Dark Count Rate (DCR)	1-3 MHz/mm ²	50-100 kHz/mm ²
Crosstalk	>40-60%	5-10%

Table 1. Comparison of basic parameters characterizing PMTs and SiPMs available in 2010 and 2015 at room temperature.

4. SiPM

For the case of application of SiPMs, SENSE identified a major scope: the achievement of a sensor capable of providing the number of photons and their arrival times which should be scalable to any area. This aim can be achieved ideally with associated electronics which should also be scalable. Ultimately, a monolithic sensor with integrated electronics would be an asset which could offer maximum flexibility for different applications.

4.1. Performance of Sensors

Producers are constantly working in developing the technology of SiPM. Major achievements can be broken down as follows:

- the reduction of the cross-talk by the introduction of trenches, improved substrate thicknesses, optimization of coating layer thickness;
- the increase of PDE:
 - by reducing the dead spaces between microcells,
 - by adopting protective materials of the microcells optimized in various wavelength regions or by removal of such layers;
 - by decreasing the device noise (i.e. DCR, optical crosstalk and afterpulsing), what allows to operate devices at much higher overvoltage, therefore higher triggering probability and higher PDE can be reached;
 - by using thin metal quenching resistors, which is almost transparent;
- reduction of dark noise;
- achievement of small size microcells with high fill factor;
- the reduction of afterpulses probability by reducing Si-impurity and the optimization of internal electrical field,
- the increase of PDE at UV region
- the reduction of signal shape variation with temperature by using thin metal quenching resistors with smaller temperature coefficient with respect to “classical” polysilicon quenching resistors (true for Hamamatsu devices);
- in monolithic arrays, the dead gap between SiPM devices was decreased down to 0.2 mm thanks to through-silicon via - TSV technology (true for Hamamatsu devices);
- reduction of temperature coefficient by optimization of epitaxial layer thickness (true for Hamamatsu devices);

In the following we outline the necessary developments aimed at improving sensor performance for the future:

- the capability of having large-area surfaces instrumented with SiPMs without degradation of performance.
- the achievement of picosecond-scale time resolutions for single photon (TOF-PET);
- the increases of PDE at:
 - infrared region (typically for car safety applications);
 - UV region (typically for Cherenkov light detection, fluorescence, etc.);
- increases of radiation hardness (typically for HEP and radiation protection applications);
- decreases of DCR, crosstalk and afterpulses would lead to:
 - higher working voltage, therefore higher triggering probability and PDE;
 - possibility to reach single photon detection at room temperature without external trigger;

For the time being, we prioritize in this Roadmap the large area development over the time resolution, which is especially useful in medical applications and in some particle-physics developments.

4.2. Readout Electronics

4.2.1. Developments in Application-Specific Integrated Circuits (ASICs) for SiPM Readout

Already several ASICs designed for SiPM readout (e.g. CitiRoC, PetiRoC, MUSIC) can be found on the market and could be coupled to the ideal sensor. Nevertheless, none of them can perfectly fulfill the demands of the ideal combination of a sensor and readout system, and therefore a dedicated effort has to be made to make these ASICs suitable for each different application. An example of this is the long tuning of EASIROC¹ to serve the ASTRI project of CTA, which became CITIROC².

The ideal ASIC should offer excellent charge resolution, an adjustable dynamic range, an excellent time resolution, a low power consumption and should have negligible dead-time even at high event rate.

An array of SiPM devices coupled to ASIC acting as multichannel readout electronics and the mother board based on a FPGA (Field-Programmable Gate Array) to control from one to few such modules together is a *semi-integrated* solution called in the following **LEGO-brick**. Following the LEGO-brick approach, an ASIC should have a fixed number of channels able to cope with the division of the sensor into readable channels. Even if the brick is 3 cm x 3 cm, it will be subdivided into sub-

¹ <http://omega.in2p3.fr/index.php/products/easiroc.html>

² <http://www.weeroc.com/en/products>

channels and the ASICs should then offer the possibility to get a single output or as many outputs as number of sub-channels. In this respect, the MUSIC ASIC³ offers an original approach as it is meant for SiPM arrays. The user can either select the sum output or the output of the individual sub-channels.

The ASIC should also integrate some slow control, such as the possibility to read the temperature of the sensor located as close as possible to the SiPM, in order to adjust the operating point when temperature changes occur.

The control of the ASIC and the trigger combination should be performed in a field-programmable gate array (FPGA) which should combine trigger signals from the different LEGO bricks to decide which event should be readout.

4.2.2. Digital sensors

A natural way to overcome the trade-off between the sensor size and its speed is theoretically the digital approach. It requires a single cell control circuitry that includes at least an active quenching, and optionally the possibility to disable/enable single micro-cells, given that the dark noise of SiPM is mostly due to a limited number of microcells. The output of the sensors is directly the number of fired micro-cells and not anymore an analogue signal which can be affected by the capacitance which increases with surface of the sensor. In a Digital system, counting photons at a given time is equivalent to check the state of the quenching circuitry of each micro-cell. While current implementations are using a multiplexing approach but still an analogue approach, *the future of digital SiPM should allow to access continuously the state of the single cells in a fast way.*

If the single cell control has many advantages, it also decreases the PDE as the fill factor decreases. This can be also tackled by using micro-lenses. Their main advantage is to focus the light into the active region of the sensor making the fill factor irrelevant. *Developing micro-lenses of high transparency is the key to have competitive PDE with digital SiPM.* Properly coated, it can also act as filter (e.g. IR filter for gamma-ray astronomy).

4.3. Integration

Nearly all applications require compact electronics. Nowadays the answer to achieve compactness in sensor and electronic integration is 3D. However, 3D is still a non-mature integration technology and may lead to low production yield and therefore high production costs at this time. For instance, currently the mobile phone manufacturer often prefers to use intermediate vertical integration where sub-components can be produced and tested separately. In this way, not only the production yield increases, but also the design flexibility. An emerging technology become widely used in communication, is the silicon or glass interposers. Having the same thermal expansion coefficient as the sensor, a compact and versatile vertical integration can be performed. Developing the glass interposers dedicated to SiPM use would offer the versatility expected from the ideal sensor.

³ "MUSIC: An 8 channel readout ASIC for SiPM arrays ", *Proc. SPIE 9899*, Optical Sensing and Detection IV, 98990G (2016);

An alternative to vertical integration of the readout electronics is the monolithic integration.-

The continuous and inexorable progress in the fields of Software, Hardware and Firmware would make possible today an innovative approach oriented to a full integration of those components with the latest generation of SiPM light sensors.

The needs of users and their applications provide the main driving force for this request. Application fields, as for example, medical, geology, biology, automotive, environmental, physics science and so on, would greatly appreciate a real effort in this direction.

Incorporating in a monolithic “block” what it is necessary to have a complete end-to-end system to be easily interfaced directly with a PC for standalone operation or a back-end electronics, in case of a more complex system, is one of the main recommendation of SENSE. The idea of building a MPDU (Monolithic Photo Detection Unit) that can perform tasks perceived as requiring by applications is an attractive one. Struggling not anymore with harness and mechanical interface to assemble different components not only will speed the system integration phase but also would remove the risk due to bad connections, missing connections, inducted electromagnetic noise and mechanical misalignment.

The MPDU is defined as the ensemble of SiPM (usually a matrix of sensors), signal processing front-end electronics and a local intelligence (FPGA or SoC FPGA).

It is believed that nowadays technology allow such level of integration. The progress in SiPM manufacturing, front-end ASIC and system integration associated with System on Chip (SoC) design gives hope that this outcome can be achieved soon.

Considering that product implementation of complex, low-power designs requires early integration of various hardware features with corresponding firmware onto one silicon device it is important to define what kind of functionality and performance are required by generic users.

The front-end signal processing is conceived for efficiently translate the SiPM analog signal in digital one. Intuitively, the goal of the signal processing is to translate the electric pulses generated by photons in the SiPM in a series of measurable pulse amplitudes sampled by analog-to-digital converter (ADC) into a numerical representation suited for further analysis. Ideally, this signal processing should yield a clean representation that is as close as possible to the user specifications.

This means that the front end should be able to handle different application needs. Some applications require detection of very intense light, some of very faint light and some other in the between. Moreover, for some applications, resolution time is mandatory. The challenge is to find the right balance and a workable solution appropriate for managing their integration within a MPDU efficiently.

A set of programmable functions, implemented through a string of configuration bits, are required to instruct the front-end on the desired operating mode. Single-photon-counting as well as charge integration should coexist and selectable by the user.

In single-photon-counting mode, a double pulse resolution of a few ns (≈ 5 ns) is enough to avoid pulses pile-up. Naturally, for the input stage, a programmable pole-zero cancellation technique is required to cope with long tail SiPM signals.

Analog chains based on fast pulse sampling or pulse height measurement technique using peak detector should be implemented including pulse-shaping time and pre-amplifier gain programmability in order to cover the desired energy dynamic range (energy measurement from 1 pe up to few thousands pe within 1% linearity should be acceptable). Internal ADC should be integrated in the MPDU in order to convert analog signals to digital data to be serially read-out.

Analog triggers (summation of analog signals) and digital triggers should be managed and selectable as well.

Fast discriminators with user adjustable threshold by means of DAC provide the digital trigger signals that are routed to a majority/topological trigger logic in the FPGA for the generation of prompt MPDU trigger. Timing measurement should also be better than 100 ps RMS jitter.

Masking of the digital triggers is also required to switch off potential noisy pixels.

An adjustment of the SiPM high-voltage should be allowed using channel-by-channel DAC connected to the ASIC inputs. That consents a fine SiPM gain and dark noise adjustment at the system level to correct for the gain non-uniformity of SiPMs.

Although current SiPM have a much lower temperature dependency than a few years ago, temperature sensors embedded in the MPDU would be useful to compensate for change in the SiPM operating voltage caused by local temperature variations.

FPGA or the last SoC FPGA devices that integrate both processor and FPGA architectures into a single device, should manage acquisition and readout. SoC devices provide higher integration, lower power, smaller size, and higher bandwidth communication between the processor and internal FPGA. They also include a rich set of peripherals, on-chip memory, an FPGA-style logic array, and high-speed transceivers.

With a SoC device the needed algorithms, data pre-analysis, readout and the full control of the MPDU could be developed quickly and efficiently.

4.4. Simulation & Modelling SiPMs

4.4.1. Numeric simulation of Geiger avalanche multiplication process in Silicon

From the known doping profile of SiPM, it's parameters like: internal electrical field, depleted region, capacitance, breakdown voltage and temperature coefficient of breakdown voltage can be obtained from numerical TCAD⁴ simulation [CITATION Nic11 \l 1033]. However, since mostly all semiconductor devices (e.g. diodes, transistors, solar cells etc.) are working below the breakdown voltage, TCAD tool is much more developed/focused on below breakdown region, while above breakdown region (i.e. normal SiPM working regime) is not yet investigated on sufficient level. Moreover, the used model for simulation of SiPM breakdown voltage includes non-physical parameters like electrons and holes relaxation times in Si. Developing the user friendly numerical simulation tool *dedicated to SiPM's*, biased above breakdown voltage would offer the prediction of such important parameter as Geiger probability (one of the parameter in PDE) as a function of interaction coordinate (i.e. light wavelength) and applied voltage.

⁴ <http://www.silvaco.com/products/tcad.html>

4.4.2. Modelling of reverse current-voltage characteristic of SiPM

To achieve the best performance for a given application, the important device parameters related to avalanche multiplication in Silicon as breakdown voltage, dark count rate, optical crosstalk and PDE have to be known. Usually these parameters are determined from dynamic measurements which require a long data taking time, quite complicated data acquisition system and precise analyzing procedure. Use of static measurements (i.e. reverse current-voltage IV characteristic) would significantly simplify the calibration and monitoring procedure but it requires good understanding of the actual shape of the IV curve. From the IV model proposed by Dinu [CITATION NDi17 \l 1033][CITATION ANa15 \l 1033] the SiPM breakdown voltage and Geiger probability can be calculated. We can expect that after further developing this model might be used for dark count rate calculation and indicate the main source of thermal noise (i.e. electrons or holes).

4.4.3. Modelling of sensor as signal source

The electrical characteristics of SiPMs have to be taken into account to properly design the front-end electronics. Therefore, a careful study of the static and dynamic characteristics of the SiPM as a signal source is required. In particular, the total capacitance and the shape of the output signal. This information can be obtained either from measurements (requires time, experimental setup, data analysis) either from proper numerical modelling (fast and simple) of SiPM`s. Presently, a few slightly different models of SiPMs are presented in the literature. First one, and the simplest one was developed for Geiger Mode Avalanche Photodiode GM-APD by Haitz [CITATION RHH64 \l 1033] and can be used to simulate a single micro-cell of SiPM⁵. More advanced model, which includes influence of all SiPM micro-cells was developed by Corsi [CITATION FCo07 \l 1033]. However, as was shown by Aguilar [CITATION JAA16 \l 1033] the Corsi model is not accurate enough to predict the exact pulse shape and especially its gain. Therefore, the further investigation of model to describe the SiPM as a signal source would be useful for community. Moreover, the parameters involved in this model should be studied and procedure for simple and fast way to determinate them should be proposed.

⁵ SiPM – is a parallel array of micro-cells on a common silicon substrate, where each micro-cell is a GM-APD connected in series with a quenching resistor

5. Classical PMTs

Currently the standard light sensors are the classical photo multiplier tubes (PMT). The SiPM, a relatively novel Si-based semiconductor sensor, is progressively substituting the PMTs in many applications, where the requirements to the sensor noise are not very stringent and a small pixel size and high amplitude and time resolutions are desired. SiPMs were discussed in the previous paragraph. In this paragraph, we will focus on the PMTs, discussing their main features as well as possible significant improvements of their performance. About 13 years ago, a research group in Max-Planck-Institute for Physics organized a PMT improvement program with the manufacturers Hamamatsu Photonics K.K. (hereafter Hamamatsu, Japan), Electron Tubes Enterprises (England) and Photonis (France) for the needs of imaging atmospheric astro-particle physics experiments. As a result, few years later, after about 40 years of stagnation of the peak Quantum Efficiency (QE) of bi-alkali PMTs on the level of 25-27%, new sensors appeared with a peak QE of 35%. These have got the name super bi-alkali. The second significant upgrade happened several years ago, as a result of the second dedicated improvement program of the PMT major parameters, this time for the needs of the Cherenkov Telescope Array (CTA). Since about two years PMTs with average peak QE of approximately 42% became available. Also, the photo electron collection efficiency of the previous generation PMTs of 80- 90% has been enhanced to the level of 95- 98 % for the new ones. The after-pulsing of novel PMTs has been significantly reduced, down to the level of 0.02 % for the discrimination threshold of 4 photo electrons (ph.e.). We will report on the PMT development and cooperation work with the companies Electron Tubes Enterprises (ETE) and Hamamatsu, showing the achieved results and giving an idea about the possible significant improvements.



Figure 1. Photo of candidate PMTs for CTA. Left: prototype test-bench PMT D872 from ETE; 2nd from left: 8-dynode PMT D569/2SA from ETE, 3rd from left: 7-dynode (final) PMT R12920-100 from Hamamatsu; 4th from left: 8-dynode PMT R11920-100 from Hamamatsu. Note that the PMTs from Hamamatsu have a mat input window.

5.1. Quantum Efficiency

The Quantum Efficiency (QE) of a PMT is defined as the ratio of the produced charge to the impinging onto the sensor flux of photons. It is a measure of sensor's photon detection ability. The higher is the QE, the higher is the probability to measure even a very low flux of photons at a high signal/noise ratio. One of the main development directions of a PMT will be to significantly enhance its QE.

5.2. The State of the Art of Quantum Efficiency in PMTs

About 20 years ago we constructed at MPI for Physics a Quantum Efficiency measurement setup (Figure 2) that consists of a) a light source box, hosting a Tungsten and a Deuterium lamps, b) a custom-modified commercial spectrometer with three different, inter-changeable gratings, c) a rotating filter wheel for suppressing the unwanted wavelengths produced by the gratings and d) a large metallic dark box enclosing the light sensor under test and e) a calibrated PIN diode of a tabulated QE for every 10nm. We illuminate the tested sensors and the calibrated diode with the wavelengths in the range of interest and measure their output currents by using the Keithley Picoammeter model 6485. In the measurement of the QE of a selected PMT we measure the current flowing between the cathode and the first dynode; rest dynodes are shorted with the first one for avoiding space charge effects that can influence measurements. The actual QE of a PMT is calculated by comparing its photo cathode current with that of a reference calibrated PIN photo diode. Typically, we illuminate $\sim 80\%$ of the area of the photo cathode and other sensors, which allows averaging possible spatial variations of the QE.



Figure 2. QE measuring custom-designed device in MPI. On left top one can see the light source (grey box) accommodating a deuterium and a halogen lamps, the small blue box is a modified spectrometer. Light from it enters into the sensor test dark box via a filter wheel. In front is shown a Keithley Picoammeter (grey) of type 6485.

In Figure 3 one can see the measured QE of three Hamamatsu PMTs together with the QE of six experimental PMT candidates for CTA produced by ETE. While the ETE PMTs show a peak QE of 35 - 38 %, the selected three PMTs from Hamamatsu show a peak QE of 41 - 43 %. The difference in QE for wavelengths below ~ 340 nm is due to the used different types of glass (Hamamatsu has used an input window glass with higher transparency in the near UV). Though different in peak QE in the spectrum range 340 - 440 nm, for wavelengths above ~ 450 nm the QE curves of Hamamatsu and ETE are not so different.

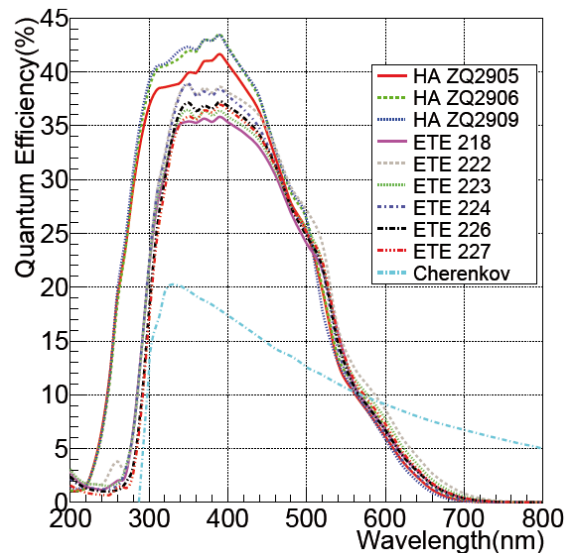


Figure 3. The measured QE of six experimental PMTs from ETE and three PMTs from Hamamatsu. The dashed curve shows the measured on Earth shape of the Cherenkov spectrum, induced by an impinging 100 GeV gamma ray.

In Figure 4 below we show the QE statistics of 300 PMTs produced by Hamamatsu in 2013. The green circles show the peak QE values while the pink circles show the result of QE curve folded with the Cherenkov spectrum.

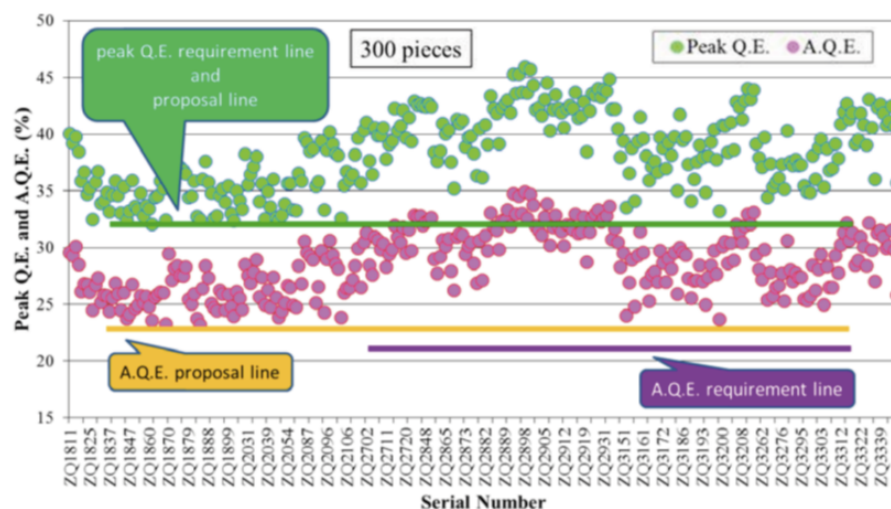


Figure 4. Peak QE of 300 PMTs produced by Hamamatsu in 2013 (green circles). The QE curve fold with the Cherenkov spectrum from 100 GeV gamma showers (pink circles) shows the average over the Cherenkov spectrum $\langle QE_{ch} \rangle$. The green and the yellow horizontal lines show the requested in the past minimum values for the peak QE and the $\langle QE_{ch} \rangle$.

5.3. Photo Electron Collection Efficiency

Only a fraction of the ph.e.s from the photo cathode will have a chance to be collected by the 1st dynode and undergo multiplication process. Some of the mis-focused ph.e.s will hit the surface of the metallic focusing plate instead of the hole in its center, and will be lost. This metallic plate is part of the electrostatic focusing system of the PMT, and is guiding ph.e.s towards the 1st dynode. The photo electron collection efficiency (ph.e.CE) on the 1st dynode is a function of the applied high voltage. Typically, the higher applied voltage between the photo cathode and the 1st dynode allow one collecting higher share of ph.e.s. For 1'-1.5' size PMTs the typical ph.e.CE is on the level of 82-88 %, wavelength dependent. These results are based on the Monte Carlo simulation of similar PMT configurations by two different PMT manufacturers. Measuring the ph.e.CE in practice is not easy; usually one obtains a measurement precision of 10-15% and this is comparable to the loss of ph.e.CE for a good PMT. Large diameter PMTs are more prone to this problem, in the past this was a well-known problem.

The main reason for this relatively low collection efficiency is hidden in the basics of the classical PMT, which is using the principle of electrostatic focusing; the manufacturer is supposed to satisfy two contradicting wishes of customers: simultaneously high ph.e.CE and a very good time resolution. The manufacturer can optimize only one of those parameters, either maximize the ph.e.CE or to provide a very good time resolution. The need to optimize simultaneously both parameters leads to a compromise solution, a bit sacrificing both the ph.e.CE and the time resolution.

In the novel PMTs for CTA the manufacturers maximized the ph.e.CE, since this is directly related to the measured charge. PMTs from Hamamatsu provide 94.6 % ph.CE for the wavelength of 400 nm. For longer wavelengths the ph.e.CE is higher, in the range of 98 %. For the wavelength of 300 nm the value of ph.e.CE is not so certain; the reason is the rest energy of the relatively energetic electron. Typically, an electron needs ~ 2 eV for getting out from the bialkali photo cathode into the vacuum, where the electrostatic field guides it towards the 1st dynode for further multiplication. A photon of 300 nm has energy of ~4 eV from which it will spend 2 eV on the so-called work-function and will fly with the rest energy of 2 eV into the vacuum. Depending on the arrival direction of the impinging photon the released electron will preferentially continue in the same direction. There is no experimental data available for this fine issue, so the manufacturers do not really know how to calculate the ph.e.CE in the near UV. For bypassing this difficulty one may assume that the ph.e. preferentially keeps the direction of the original photon but has the usual cosine law angular distribution around it. Such simulations showed that the ph.e.CE for 300 nm could be as high as 88 %.

For achieving the above listed unusually high ph.e.CE efficiencies it is necessary operating PMT at a high photo-cathode to 1st dynode voltage of ≥ 350 V. Obviously when changing the HV of the PMT one will change also the photo-cathode to 1st dynode voltage thus deteriorating the ph.e.CE. For avoiding this one can stabilize the applied voltage between the photo cathode and the 1st dynode.

We want to note that the ph.e.CE is a more complex issue for strongly curved or hemispherical PMT input window shape than for the flat one. In PMTs of hemispherical shape input window, for example, the ph.e., which is kicked out from a large distance from the center, i.e. at a large azimuth angle (this we define as the angle between the longitudinal axis of the PMT and the photon impinging direction), has a relatively high chance to land on the focusing metallic electrode and get lost.

5.4. Photon Detection Efficiency

The essential parameter of any given light sensor is not the QE but its Photon Detection Efficiency (PDE). PDE is the convolution of the wavelength dependent QE with the wavelength dependent ph.e.CE:

$$PDE(\lambda) = QE(\lambda) \times \text{ph.e.CE}(\lambda)$$

Because the phCE(λ) is always ≤ 1 , as a rule the PDE(λ) is less than the QE(λ).

An absolute measurement of the PDE is not easy, uncertainties of several measured parameters make it difficult to perform a precision measurement.

The *parametric down conversion* is an elegant and very precise method for measuring the PDE but because of the “splitting of one photon into two” usually it is limited to relatively long wavelengths. It is a costly and complex issue to provide a laser beam of a very deep UV wavelength and to find an appropriate non-linear crystal.

Unlike the absolute measurement it is relatively easy to perform a relative measurement between given sensors. One just needs to provide identical light fluxes on the given sensors under identical geometries. After that one only needs to compare the measured numbers of ph.e.s.

5.5. First Dynode Amplification: A Key to Amplitude Resolution

Note that the high applied voltage not only provides high PhEC efficiency but also a high signal/noise ratio because of large number of secondary ph.e. kicked out from the 1st dynode. Typically within some given range, up to several hundred of Volts, there is proportionality between the applied photo cathode to 1st dynode HV and the number of kicked out secondary electrons. This provides a high signal to noise ratio and high amplitude resolution. The rest dynode system plays only a secondary, moderate role in signal to noise ratio of the total amplification chain, see the equation (1) below; note that the 2nd term in the sum is much less than the 1st term:

$$\text{var}(G) = \text{var}(g_1) + \text{var}(g) \cdot \langle g \rangle \cdot [\langle g_1 \rangle \cdot (\langle g \rangle - 1)]^{-1} \quad (1)$$

In above formula *var* stands for the relative (normalized to gain) variation, *G* for the gain of the PMT, g_1 for the gain of the 1st dynode and the $\langle g \rangle$ for the gain of rest dynodes (under assumption that they have the same gain).

Above several hundred Volts applied between the photo cathode and the 1st dynode, the number of released secondary electrons may saturate and no further gain can be achieved. Instead, the rate of after-pulsing may increase. So typically there is an optimum applied voltage range where the gain of the 1st dynode and the PhEC efficiency are close to maximum while keeping the after-pulsing rate below a given level.

Summarizing one can say that stabilization of applied voltage between the photo cathode and the 1st dynode is necessary

- for keeping a constant gain of the 1st dynode,
- for providing a high PhEC efficiency
- for high amplitude resolution of the PMT
- for constant and high time resolution.

5.6. Transit Time Spread

Ph.e.s from different locations on the photo cathode surface move over somewhat different paths until most of them land somewhere on the surface of the 1st dynode. These path differences, along with additional path differences when amplified by the dynode system, cause small time differences which can be characterized by using the parameter electron Transit Time Spread (TTS). As mentioned above, the manufacturer is designing the front focusing chamber of the PMT aiming to optimize the PhEC efficiency and the TTS. It is not possible to simultaneously satisfy both conditions.

5.7. Afterpulsing

This effect is mostly due to impact ionization of the atoms of certain chemical elements as well as due to light emission from the dynodes, which are bombarded by accelerated energetic electrons. The latter impinge onto the dynodes sometimes ionizing and releasing adsorbed on the surface chemical elements as well as they can interact with the atoms and molecules of the rest-gas in the vacuum tube. In this type of after-pulsing the positively charged ions move in the opposite to electrons direction, part of them reaching the photo cathode and, due to big momentum of heavy ions, releasing bunches of electrons. Obviously at least ~ 2000 times heavier ions (H⁺) collect the same energy as the electrons but because they are much heavier, they need more time for this reverse-travel. Typically an H⁺ ion moving in a potential field of 300 V between the photo cathode and the 1st dynode, which are separated by ~30 mm, will be delayed by ~ 300 ns compared to the impacting electron. This process reminds a simple mass-spectrometry, i.e. the heavier the ion, the longer it will need to reach the photo cathode.

Typically the delay scales as \sqrt{M} (for one-time ionized ions), where M is the mass of the heavy ion in units of H atom mass.

In contrast to the above described mechanism, the light-induced after-pulsing is much faster; the system of dynodes reminds a kind of light guide. True, it is a poor light guide because of the usually dark color coating of the dynodes.

Because of the relatively short distances in a PMT, the delay of the light-induced pulse is mainly due to the travel time of the electrons, typically to the late dynodes where they can generate a relatively high intensity light. Typically, these pulses appear, depending on the topology and the size of a given PMT, in the range of 20-25 ns after the main, impinging onto the photo cathode pulse.

5.8. Single Photo Electron Peak to Valley Ratio

This is one of the important parameters of PMT, which describes how good a given PMT can detect single ph.e. events. Usually a PMT with the first dynode gain of ≥ 6 will show a peak in the output amplitude distribution. This peaked distribution can be characterized in different ways. One way, coming as a heritage from the past, is for the given data set to take the ratio of the frequency of the peak to that of the valley in amplitude distribution. The higher is this ratio, the better can a PMT discriminate single ph.e.s from noise. In the not so far past, regular PMTs showed a peak/valley ratio of 1.2-1.8; these were considered as relatively good sensors. Nowadays PMTs with much higher peak/valley ratio became available.

The new PMTs developed for the CTA project have a substantially higher peak/valley ratio, in fact they became almost “quantacons”; peak/valley ratios of $\geq 2.5 - 3.0$ became usual.

5.9. Influence of the Earth’s Magnetic Field on the PMT Gain

The geomagnetic field of Earth bends the trajectories of electrons moving towards the dynodes, especially those moving towards the 1st dynode. This effect will depend on the latitude of the location which is related to the magnetic field strength. Obviously, it is also a function of the orientation of the PMT relative to the magnetic field lines. This force is at maximum when the magnetic field is perpendicular to the direction of motion of electrons. Wrapping a PMT into mu-metal tube can significantly reduce its sensitivity to the geomagnetic field.

5.10. Typical Achieved Parameters for the recent Generation of Small-Size PMTs

It is interesting to show the space of parameters that have been achieved for the recent generation of best PMTs. For illustration purposes we show below measurements of some of the important parameters achieved for the 1.5' size PMTs of bialkali photo cathode from the ETE and Hamamatsu companies. Figures 5-8 show the dependence of the gain versus the applied HV for 7 and 8 dynode Hamamatsu PMTs, the pulse width versus the applied HV for Hamamatsu and ETE PMTs, the pulse width versus the gain for Hamamatsu and ETE PMTs as well as a screenshot from a fast oscillograph showing the pulse shape of a 7-dynode PMT from Hamamatsu, correspondingly. The summary of the achieved technical parameters for the 7-dynode PMT R12992-100 from Hamamatsu are shown in Table 2.

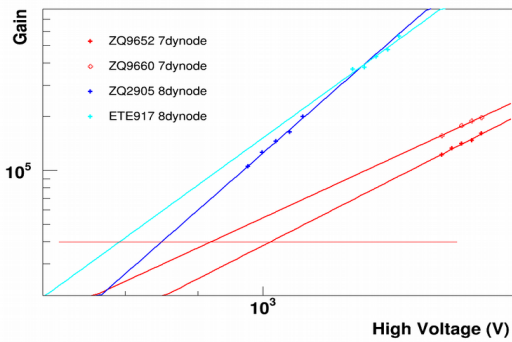


Figure 5. Gain versus applied HV for the Hamamatsu 7-dynode and 8-dynode PMTs.

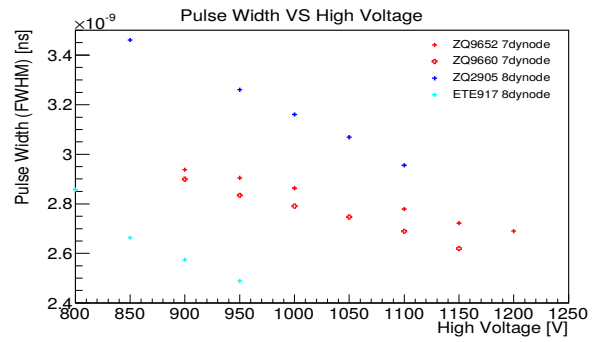


Figure 6. PMT pulse width versus applied HV distribution for Hamamatsu and ETE PMTs.

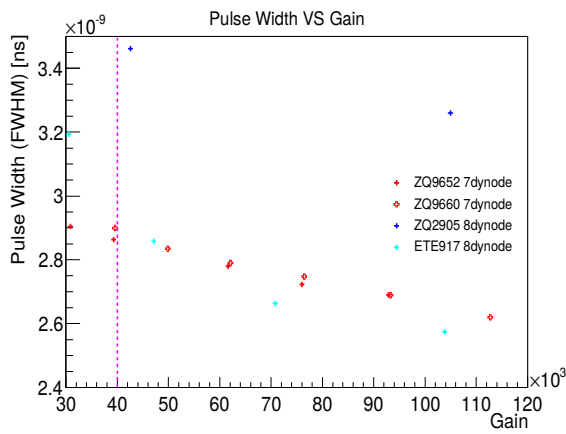


Figure 7. PMT pulse width versus gain (applied HV) for Hamamatsu and ETE PMTs.



Figure 8. Pulse width of a Hamamatsu 7-dynode PMT operated under 1000 V.

TECHNICAL INFORMATION

TENTATIVE

Feb. 2014

R12992-100

For Gamma-ray Telescope (CTA project), Fast time response, CC window
38 mm (1.5 inch) Diameter, Super Bialkali Photocathode, 7-stage, Head-On Type

GENERAL

Parameter		Description / Value	Unit
Spectral Response		300 to 650	nm
Peak Wavelength of Cathode Radiant Sensitivity		400	nm
Window	Material	Borosilicate glass	-
	Shape	Concave-Convex (R20)	-
Photocathode	Material	Super Bialkali	-
	Minimum Effective Area	30	mm dia.
Dynode Structure / Number of Stages		Linear Focused / 7	-
Base		JEDEC No.B12-43	-
Operating Ambient Temperature		-30 to +50	°C
Storage Temperature		-80 to +50	°C
Suitable Socket		E678-12A (option)	-

MAXIMUM RATINGS (Absolute Maximum Values)

Parameter		Value	Unit
Supply Voltage	Between Anode and Cathode	1500(TBD)	V
	Between Cathode and 1 st Dynode	400	
	Between Anode and Last Dynode	250	
Average Anode Current		0.1	mA

CHARACTERISTICS (at 25 °C)

Parameter		Min.	Typ.	Max.	Unit
Cathode Sensitivity	Luminous (2856 K)	-	100	-	μA/lm
Cathode Blue Sensitivity Index (CS 5-58)		-	13.5	-	-
Radiant Sensitivity (at peak wavelength)		-	110	-	mA/W
Quantum Efficiency	at peak wavelength	32	35	-	%
	from 300 nm to 450 nm	25	-	-	
Collection Efficiency (at 400 nm, simulation)**		-	95	-	%
1 st Dynode Gain		6	10	-	-
Anode Sensitivity	Luminous (2856 K)	-	4	-	A/lm
Gain		-	4x10 ⁴	-	-
Single Photon Counting Peak to Valley Ratio		1.8	2.5	-	-
Anode Dark Current (after 30 minute storage in darkness)		-	5	20	nA
After Pulseing (threshold 4 p.e. and Gain 4x10 ⁴ voltage)		-	0.02	-	%
Anode Pulse Rise Time**		-	2.5	-	ns
Anode Pulse Width (FWHM)**		-	-	3.0	ns
Electron Transit Time**		-	22	-	ns
Transit Time Spread (FWHM with single p.e.)**		-	-	2.0	ns
Pulse Linearity (+/- 2 % deviation)		15	20	-	mA
Life (50 % drop in Gain)		200	-	-	C

NOTE : Anode characteristics are measured with a voltage distribution ratio and supply voltage shown next page.

(** Collection efficiency and time response are defined with effective area of 30 mm in diameter.)

HAMAMATSU
HAMAMATSU PHOTONICS K.K. Electron Tube Division

Table 2. Technical specification of the 7-dynode, 1.5' PMT R12992-100 from Hamamatsu.

6. SENSE Contributions to R&D of Sensors

6.1. SENSE Contributions to SiPMs

6.1.1. Performance of Sensors

In SENSE we work at qualified laboratories at Ideasquare (CERN), Catania, Nagoya, KIT and Heidelberg in order to characterize sensors and to define measurements procedures, cross-check results and the associated errors. In particular, we concentrated on cross-check of PDE (as a function of overvoltage ΔV and wavelength λ) and optical crosstalk. Up to date, the measurements were done and results compared for five different devices produced by Hamamatsu:

- Hexagonal devices produced for CTA SST-1M telescope: LCT2-S10943-2832;
- four latest devices, from first and second generation of so-called low voltage reverse LVR series: LVR-3050CS, LVR-6050CS, LVR2-6050CS, LVR2-6050CN.

The experimental set ups at Unige, Nagoya and Catania can be used to measure different SiPM parameters like: breakdown voltage, gain, dark count rate, optical crosstalk, afterpulses probability and photon detection efficiency at various wavelengths. As an example, the results for an LVR-3050CS device obtained by University of Geneva/Ideasquare, Catania Observatory and University of Nagoya are presented in Figure 9 ÷ Figure 12. We can observe a good agreement between PDE obtained by three partners. The difference between results from UNIGE and Catania is inside the experimental errors and between Catania and Nagoya is around 7%. This difference is related to systematic error in calibrated SiPM which was used by Nagoya to calculate the absolute light flux reaching SiPM.

In the same time, significant (up to 100% between data from Catania and Nagoya) difference in optical crosstalk was found. This difference led to the improvement on measurement setups and better understanding of found results. It was found that, this difference is related to pile-up effect, which is found to be significant if low crosstalk should be measured. To reduce a pile-up effect a new measurements at much higher bandwidth were performed (1 GHz instead 20 MHz) as well as an off-line correction procedure was applied. The new results are presented in Figure. 12 We can observe only 7% relative or < 3% absolute difference between results obtained by University of Geneva and Nagoya University. The experimental set up used by Catania observatory is not able to decrease or remove pile-up effect due to fixed shaping time. Therefore, the results presented by Catania should be interpreted as a superposition of optical crosstalk and pile-up effect from thermally generated pulses and noise from read-out electronics.

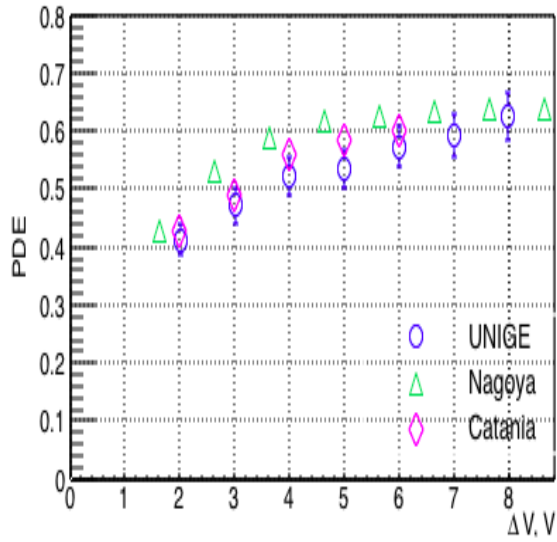


Figure 9. Cross-check of PDE as a function of Overvoltage at 405 nm wavelength, between three partners.

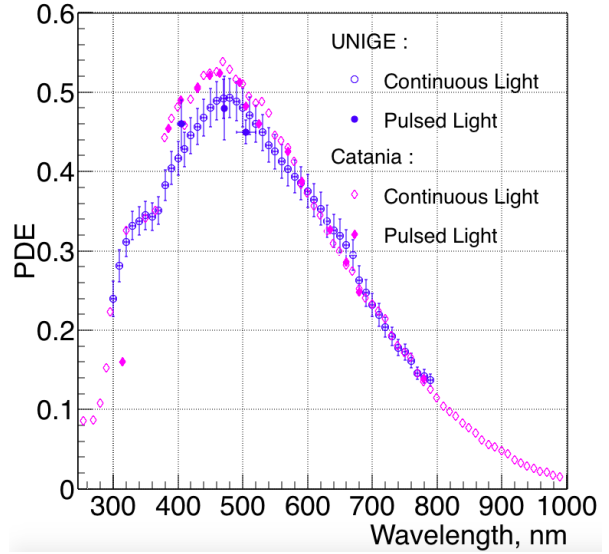


Figure 10. Cross-check of PDE as a function of wavelength at 3 V overvoltage. Results were obtained by University of Geneva and Catania Observatory.

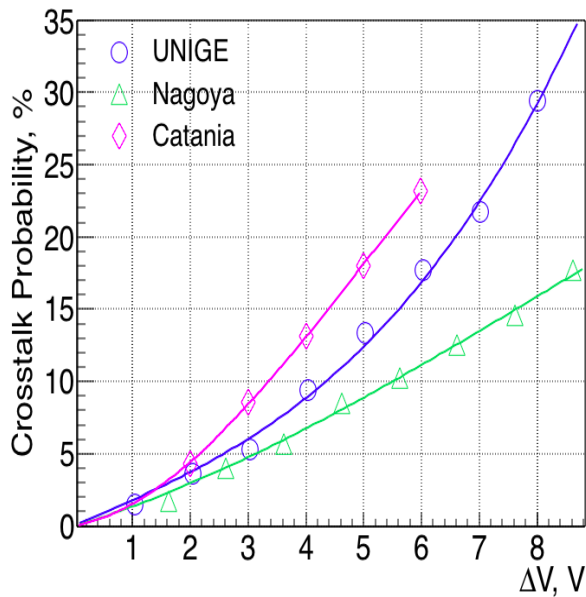


Figure 11. Cross-check of P_{XT} as a function of Overvoltage, between three partners first results.

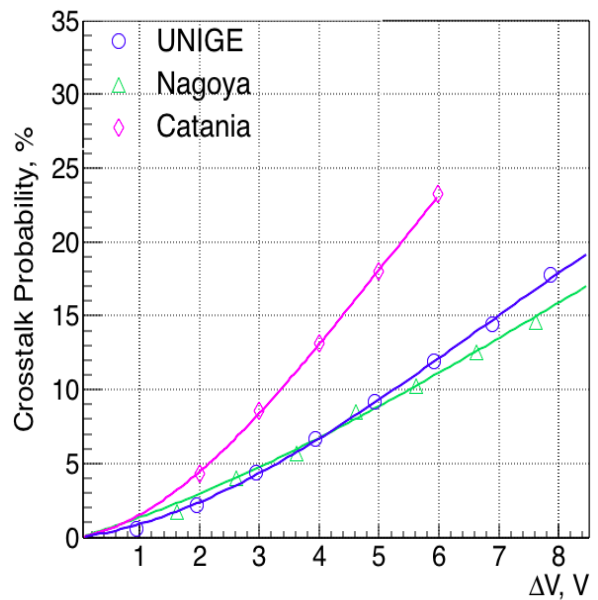


Figure 12. Cross-check of P_{XT} as a function of Overvoltage, between three partners, improved results.

6.1.2. Matrices of SiPM

Matrices of SiPM of different integration level are available from a few companies. While some of them offer only a closely-packed sensor area, others offer also some integrated electronic solutions. We believe that the future of SiPM-based imaging devices belongs to highly integrated, modular matrices of SiPM that even for ns fast signals will resolve multi- photo electron (ph.e.) signals, will show low sensitivity to temperature and power supply instabilities, can operate at a practical absence of cross talk and after-pulses ($\leq 1\%$) and moderate dark rate at room temperature. Such matrices can have a PDE of as high as $\geq 65\%$ for the interesting for many applications wavelength range (300-700)nm, could have very low dead area and allow one, as *lego* bricks, to assemble a fully buttable imaging device that has all the necessary electronics below the area covered by the chip front size. By means of the 3D design and packaging such chips can allow one to obtain an extremely close spacing of sensors a mosaic and construct very high resolution imaging cameras of arbitrary size and shape. This is what one needs in scientific, medical and really diverse technical applications.

It is a very challenging goal to develop large size, sensitive (also in the near UV) sensors of very high PDE, substantially exceeding that of the state of the art classical PMTs. For achieving very high PDE one needs to operate the SiPM under very high, close to saturation Geiger efficiency. For this one needs to apply a high relative over-voltage (defined as $\Delta V/U$ where $\Delta V = U(\text{applied}) - U(\text{breakdown})$) to the sensors, which means operating them under very high gain ($Q = C \times \Delta V$ where C is the capacitance and ΔV is the over-voltage). On the other hand, light emission in SiPM, responsible for the adverse effect of the cross-talk (hereafter X-talk), is proportional to the number of electrons in the avalanche, i.e. to the sensor's gain. As a consequence of high gain one will have a high-level of X-talk that deteriorates the amplitude and the time resolutions of the SiPM. One can clearly see the controversial requirements: for high PDE one needs a high Geiger efficiency and as a consequence one operates at high gain, but for low level of X-talk one needs a low gain. It is impossible to simultaneously satisfy both requirements. An intermediate solution could be operating SiPM at a relatively low value of PDE that will provide a relatively low X-talk (and noise). But this solution, in the past used for operating SiPM such, for example, as the MPPCs from Hamamatsu, provides a working point on the strongly varying (rising) part of the PDE curve versus the applied over-voltage. That makes the device strongly dependent on the applied over-voltage and the operating environment temperature (variation of temperature changes the breakdown voltage. Thus at a constant applied voltage the over-voltage follows the changes of the breakdown voltage, varying the PDE and the gain).

The situation with X-talk is more pronounced for large cell size SiPMs that potentially can provide the highest possible geometrical efficiency and the maximum PDE needed in "photon-hungry" applications. Typically a SiPM cell of $(100 \times 100) \mu\text{m}^2$ size correspondingly has a 4- and 16-times larger area and capacitance than the $(50 \times 50) \mu\text{m}^2$ and $(25 \times 25) \mu\text{m}^2$ ones. For the same applied over-voltage the larger capacitance means a higher charge. Consequently, a SiPM that is based on large size cells will have a higher level of light emission and thus will produce higher X-talk. This means that especially for large cell-size SiPMs the X-talk is a serious concern. The logical consequence is that only at the cost of strong suppression of the X-talk one can operate a SiPM under maximum PDE.

Currently SiPM are available that almost fulfill the above conditions, i.e. they show a very competitive PDE at a high gain and a relatively low level of X-talk. These are mostly SiPM based on the cell size of $\sim 50\mu\text{m}$. The chip size is typically $3\text{mm}\times 3\text{mm}$ or the double of it, $6\text{mm}\times 6\text{mm}$. A very interesting question is where the size limits are.

From the above text it is clear that producing SiPM chips of size significantly larger than 10mm is a very challenging task. Besides, even if it is doable, these will be slow devices.

Imagine one needs to cover with such SiPMs a detector area of $\sim 1\text{m}\times 1\text{m}$. Of course one can build such an imaging camera with a lot of manual work and optimization. By assuming the above mentioned sensor sizes, one will need to use 30-100 thousand sensors and a corresponding number of readout channels. So it is obvious that organizing readout for $\sim 100\text{k}$ channels is possible but it will cost very much time, finances and human efforts; it is a very challenging task.

There are tasks where the very high resolution offered by SiPM will not be the primary issue; in this class of tasks it is rather to have a large detector area with moderate resolution of say, for example, several mm to a few tens of mm. This can be achieved by summing up the outputs of many SiPM. This summing up shall be done in such a way that the output capacitances of the SiPM chips will not add together; in contrary, if this happens, then the device will show only a low bandwidth and it can be used only in relatively slow applications. For the desired effect the outputs of the SiPMs shall be "isolated" from each other and only then put into a sum. Such a solution has been pursued by our institute for constructing composite SiPM pixels, which are since May 2015 installed in the MAGIC-I telescope imaging camera and currently are under extensive tests.

A very challenging task is to find out where the size limit of such SiPM-based composite pixels are; what are the main limiting factors, when essentially without sacrificing the speed of the sensors one can construct large active surface area detectors.

In the ideal case one would desire to produce the sum-signal from the user-defined selected number of SiPMs with or without keeping the intrinsic resolution offered by a single SiPM chip. This could be a solution based on multiple SiPMs within a given size say, for example, one or two-inch size matrix, where the user can define by software the needed spatial resolution and the minimum integration size. These composite pixels will need a full data processing electronics being designed (or installed) behind the active full area of the chip.

By using such multiple composite pixels, one will have the possibility to construct imaging surface area of any desired resolution, size and shape just by assembling them next to each other, like a **LEGO Brick** (See Section 4.2.1).

6.1.3. The D-LIGHT development

The D-LIGHT is a new concept of hybrid sensor mixing the advantages of analogue and digital sensors. Digital SiPMs have been introduced and patented by Philips PDPC but the technology has to be modified in order to fulfil requirements of fast readout typical to particle and astroparticle physics detectors.

This kind of sensors should have a single cell control circuitry, which should be somehow also programmable. By tuning the cell response, the dynamic range, the timing performance of the device can be tailored to a specific application.

At the same time the idea is to use a different approach for its readout. In standard digital devices, as also in the Philips Digital SiPM, each cell is readout individually. This cannot be done in parallel and then a serial readout, using multiplexing is performed. This clearly introduces a dead time, which also scales with the number of cells.

Here and hybrid approach is proposed in which the output signal is like an analog standard device, but can contain all the information on the number of fired cells and they relative time. This information can be the extracted by the electronics readout which will then output a list on photon and their relative time.

At a first stage the hybrid sensor would provide the timing of each photons thanks to the SAMPIC ASIC offering possibility timing resolution lower than 10 ps. As an ultimate goal the 3Dplus know-how would allow to perform a custom 3D integration of the sensor, the readout ASIC and the FPGA used to control them. A proper use of the ASIC and a smart programming of the FPGA would allow any user to access in real-time the number of detected photons and their time distribution.

A monolithic integration of sensor and of the readout part implemented in the separate ASIC would be the next generation of *semi-integrated LEGO-brick* (See section 4.2.1), which could be assembled with others to build a large tile which will be read and controlled as a single channel.

6.2. SENSE Contributions to PMTs

Photomultiplier Improvements:

Improve photon detection efficiency:

CsI photocathodes can achieve a peak quantum efficiency of 80%, but no visibly light sensitive photocathode comes close to this value. A principle reason for this difference is the crystal structure of CsI – this material is available with grain size much larger than the electron transport distance to the surface, basically eliminating grain boundary scattering. We propose to engineer heterojunction photocathodes using modern materials science techniques. There has been significant progress in the growth of alkali antimonide photocathodes for accelerator application based on in situ x-ray analysis of materials during growth. This progress charts a clear path toward higher QE performance for these materials – by growing material without grain boundaries – and potentially with complex material junctions to optimize for charge transport (in a manner similar to InGaAs:GaAs:GaAsP heterojunctions). Development in this area will include both modelling of material performance and demonstration of growth techniques capable of realizing heterojunction growth. There is a significant synergy in this area with other technological and scientific applications of this class of materials, making progress potentially of broad-reaching impact.

Other materials-based improvements of photocathode performance are also desirable – particularly addressing degradation due to ion bombardment. This can potentially be addressed by a combination of material crystal structure and device design.

Multiplex Photomultipliers/ improve spatial resolution of single photon detection:

While achieving position resolution for arrays of SiPMs is routine, traditional photomultipliers do not provide equivalent capability. Microchannel plate based devices such as the Photonis Planacon provide position resolution, but are quite expensive and cover relatively small area (5x5 cm²). A large area, single photon sensitive, photocathode based sensor would be desirable. One method of achieving this goal is the Timed Photon Counter being developed by Delft University and Nikhef. This device relies on transmission dynodes to achieve gain, allowing the charge to be read out via a pixel chip – effectively multiplexing the PMTs and providing spatial resolution of 10's of microns. This design could be expanded to provide larger pixels, with the dynodes also acting as electron funnels.

7. Strategy

7.1. SiPM

Within the frame of SENSE, we are discussing the possibility of further major improvements of the main parameters of SiPM, such as enhancing its PDE and reducing the cross talk well below the 1 % level. It seems that we have the right ideas for the possible design, which of course need to be discussed and further investigated in greater detail. We are thinking that the frame of SENSE provides a very good foundation for these studies and discussions, which in the end could outline one of the main directions of the Roadmap. The further characterization of SiPM device (with improved PDE and cross talk) can be done at experimental set up at Unige, Nagoya or Catania, since these set ups have been already cross calibrated for these kind of measurements.

The other direction that we would like to pursue in our studies is related to the simple but almost universal fast readout for the composite clusters of SiPM. Imagine a one or two-inch sized matrix of composite SiPMs, connected to a low-cost ASIC on its rear side, which includes a nanosecond-fast trigger and a full chain of readout electronics. The specialized ASIC shall allow the user to select and measure under computer control signal either from the outputs of individual SiPMs or from an arbitrary sum of the signals from a desired number of SiPM in the matrix. In this way, we hope one can arrive at a “universal” unit, which can be considered as the basic “brick” for constructing imaging cameras of arbitrary size, by simply assembling them as a *semi-integrated LEGO-brick*. Development of such a SiPM matrix and of the ASIC could be the other major directions to be followed by the SENSE Roadmap. David Gascon from ICCUB//SiUB group from University of Barcelona is working on flexible ASIC based front end read-out electronics for photosensors and he is on the way to sign the Cooperation agreement with SENSE. The development of such *semi-integrated LEGO-brick* will obviously have a high innovation potential for all applications ranging from a scientific impact in astroparticle and particle physics as well as in medical diagnostics to a multitude of other technical applications. All areas of application shall economically benefit from a coordination of the development of a **LEGO-brick** like array of SiPMs with integrated readout electronics.

The last direction that we would like to follow is the D-LIGHT. D-LIGHT is the hybrid SiPM sensor which includes advantages from both analogue and digital SiPM devices. In D-LIGHT hybrid approach the output signal is like an analog standard device (sum of fired cells), but can contain all the information on the number of fired cells and they relative time. This information can be then extracted by the readout electronics which will then output a list on photon and their relative time. At a first stage the hybrid sensor would provide the timing of each photons thanks to the SAMPIC ASIC offering possibility timing resolution lower than 10 ps. As an ultimate goal the 3Dplus know-how would allow to perform a custom 3D integration of the sensor, the readout ASIC and the FPGA used to control them. A proper use of the ASIC and a smart programming of the FPGA would allow any user to access in real-time the number of detected photons and their time distribution. Unige can contribute in ASIC and interface to high performance developments as well as provide and access to probe station and flip-chip machine.

7.2. PMT

In Error: Reference source not foundTable 3Error: Reference source not found we show the parameters of the contemporary best PMTs with semi-transparent photo cathode. Though these can satisfy the most demanding requirements in diverse application, still the peak QE is “only” ~ 40 %. Note please that only about half of the impinging photons interact with the thin photo cathode, typically of ~25 nm thickness. The rest of the light simply passes through the photo cathode.

Property	Acronym	Condition	Value
Peak quantum efficiency	Peak QE	Within 290-600nm	~ 35 - 43 %
Ph.e. collection efficiency on the 1 st dynode	Ph.e.CE	400nm, cathode to 1 st dynode HV=350 V	94.6 %
Operational gain	Gain	Nominal gain	40000
Afterpulsing probability	AP	≥ 4 ph.e., nominal gain	≤ 0.02 %
Pulse width	σ_{width} FWHM	40k gain @ HV=1000 V	≤ 3 ns
Excess noise factor	F-factor	40k gain @ HV=1000 V	≤ 1.10
Transit time spread	TTS, FWHM	single ph.e., HV=1000 V	≤ 1.6 ns
Rise time	σ_{rise}	40k gain @ HV=1000 V	≤ 2.5 ns
Single ph.e. amplitude resolution	single ph.e. res.	8 $\frac{\sigma}{\mu}$ above amplifier noise	~45 %
Linear dynamic range (with CW)	LDR	minimum 1 ph.e.	5000 ph.e.
Ageing of dynode system	<i>Fatigue</i>	Arriving at half gain	200 C

Table 3. Main characteristics of best bialkali PMTs as of today.

In a very simplified scenario one may imagine that a) all the impinging photons can interact with the photo cathode (a significantly thicker layer will do that). Let us further imagine that all the produced electrons could travel b) without energy loss towards the photo cathode - vacuum boundary (low scattering losses on phonons and an imaginary electric field gradient inside the photo cathode could make it). Now, c) if these electrons could be released into the vacuum, where the electrostatic field will guide these to the 1st dynode, one will essentially double the QE. Though this sounds not more than an oversimplified “Gedankenexperiment”, the essential to be solved problems for enhanced QE can be clearly outlined.

In the frame of the SENSE project we are trying to define the roadmap that shall allow one to systematically solve the above outlined a), b), c), +... problems, moving towards the PMTs with significantly enhanced (double?) QE.

The future PMTs with double QE will make a major impact on research, industry and medicine applications.

7.3 Milestones

Here we highlight the major milestones SENSE aims to achieve for PMTs and SiPMs.

PMTs.

- Try to improve the understanding of the bulk properties of bialkali photo cathode material as a semiconductor
- Move towards engineering heterojunction photocathodes using modern materials science techniques
- Growing materials without grain boundaries – and potentially with complex material junctions to optimize for charge transport, also by considering ion implantation
- Pursue further improvements of transmission dynodes

SiPMs.

- Understand the potential of further improving the major parameters of SiPMs as sensors, outline the possible developments, also interactions with possible industrial partners
- Give contours to a “standard” brick of the SiPM-based sensor of one or two-inch size
- Move towards the SiPM “standard brick” with “universal” fast readout scheme, a first step towards the “Lego” principle for assembling imaging cameras of arbitrary size
- Move further from semi-integrated standard brick to fully integrated LEGO-Brick through implementation of 3D integration

8. Summary

This Roadmap represents not only a significant milestone, but also a benchmark for the future development of the ultimate low light-level sensor. While the creation of this plan required significant effort and commitment from many entities, it is only the beginning. Much work lies ahead to implement the strategies laid out in this document. Coordination and collaboration among SENSE, academia and industrial partners will be essential to moving the R&D forward. The strategies outlined in this Roadmap will require immediate attention to ensure their ultimate success. If everything comes together in support of this plan, and its key elements are implemented, SENSE is confident the dream of an ultimate LLL sensor will become a reality.

9. Bibliography

- A. Nagai, N. D. (2015). Breakdown voltage and triggering probability of SiPM from IV curves. 1-4.
- F. Corsi, A. D. (2007). Modelling a silicon photomultiplier (SiPM) as a signal source for optimum front-end design. *Nuclear Instruments and Methods in Physics Research A*, 572, 416-418.
- Haitz, R. H. (1964). Model for the electrical behavior of the micro-plasma. *Journal of Applied Physics*, 35, 1370-1376.
- J.A. Aguilar, W. B. (2016). The front-end electronics and slow control of large area SiPM for the SST-1M camera developed for the CTA experiment. *Nuclear Instruments and Methods in Physics Research A*, 830, 219-232.
- N. Dinu, A. N. (2017). Breakdown voltage and triggering probability of SiPM from IV curves at different temperatures. *Nuclear Instruments and Methods in Physics Research A*, 845, 64-68.
- Nicola Serra, G. G. (2011). Experimental and TCAD Study of Breakdown Voltage Temperature Behavior in n+/p SiPMs. *IEEE TRANSACTIONS ON NUCLEAR SCIENCE*, 58, 1233-1240